ISSN 1225-8024(Print)
ISSN 2288-8403(Online)

한국표면공학회지
J. Korean Inst. Surf. Eng.
Vol. 51, No. 1, 2018.
https://doi.org/10.5695/JKISE.2018.51.1.79

<연구논문>

Formation of $CH_3NH_3PbBr_3$ Perovskite Nanocubes without Surfactant and Their Optical Properties

Artavazd Kirakosyan[a], Seokjin Yun[a], Deul Kim[a], and Jihoon Choi[a,*]

[a]Department of Materials Science and Engineering, Chungnam National University, Daejeon, South Korea

(Received December 16, 2017 ; revised January 19, 2018 ; accepted January 21, 2018)

ABSTRACT

We systematically investigated the optical properties of sub-micron sized methylammonium lead tribromide ($CH_3NH_3PbBr_3$) cubes in the range of 100 to 700 nm, which were prepared by a surfactant-free precipitation method. We found that despite the strong absorbance, their photoluminescence quantum yield (PLQY) is very low as 0.009~0.011 % for whole range of sizes. Surfactant-free synthesis approach results in nanocubes that has no surface passivating reagents (e.g. surfactants) on their surface. As-prepared particles contain a large number of surface defects that may cause the low PLQY. The role of the surface defects were investigated in their photoluminescence decay process, which can be correlated with the particle size. Larger particles are characterized by a slower decay rate compared to smaller particles due to a large number of surface defects in the smaller particles that trap more excitons in the fluorescence decay process. These experimental results provide new insights into the fundamental relationship between surface state and optical properties.

Keywords : $CH_3NH_3PbBr_3$, Methyl ammonium lead bromide, Luminescence

1. Introduction

During recent several years the organohalide lead perovskite materials, particularly methylammonium lead tribromide ($CH_3NH_3PbBr_3$; $MAPbBr_3$), have shown a promising potential for their applications in photovoltaics and light emitting diodes owing to their wide range of tunnability in optoelectronic properties that can be achieved by a control of their composition, dimension, and morphology [1-5]. The band-gap of $MAPbBr_3$ is demonstrated to be tuned in wide range (1.6~2.3 eV) by a composition control where Br^-, Pb^{3+}, and MA^+ were partially substituted by either Cl^- or I^- anions, Sn^{3+}, and organic cations (i.e. formamidinium, ethyl ammonium), respectively [6-8]. Additionally, the optoelectronic properties of layered $MAPbBr_3$ can be tuned by reducing the particle thickness to nanometer levels comparable to exciton Bohr radii, where the quantum confinement (QC) affects their band gap energy. Nanoplatelet of $MAPbBr_3$ with a different number of layers in nanometer ranges can be successfully synthesized by a ligand-assisted exfoliation (top-down synthesis) [9] or ligand controlled synthesis (bottom-up approach) process [10].

The surface state of $MAPbBr_3$ perovskite materials in the nanoscale dimension (i.e. 0-D nanosphere, 1-D nanowire, 2-D nanoplatelets) plays a critical role in their colloidal stability as well as optoelectronic performances. Dangling bonds on the surface of nanoparticles introduce a defect energy level that quenches the exciton and reduces the photoluminescence quantum yield. The surfactant molecules bind to these dangling bonds and eliminate the trapping sides on the surface, and thus enhance their optical properties [11]. Moreover, the surfactant molecules absorbed on the surface are considered as a protecting barrier for their colloidal and morphological stability. Amine molecules are commonly used as a surfactant for $MAPbBr_3$ perovskite nanoparticle synthesis. Kim

*Corresponding Author: Jihoon Choi
Department of Materials Science and Engineering, Chungnam National University
Tel: +82-42-821-6632 ; Fax: +82-42-821-5850
E-mail: jihoonc@cnu.ac.kr

et al. demonstrated a fluorescence chemosensor based on $MAPbBr_3$ nanoparticles coated by *n*-octylamine to detect different aliphatic alkyl amines. $MAPbBr_3$ nanoparticle-cast film demonstrates fast quenching behavior [12]. Muthu et al. used $MAPbBr_3$ to detect 2,4,6-trinitrophenol (TNP, picric acid) in a liquid and vapor state where strong electron affinity and hydrogen bonding leads to their photoluminescence quenching enabling selective detection [13]. Typically, the surface passivation of $MAPbBr_3$ with a surfactant molecule is performed during the synthesis process at the initial stages of nuclei formation; the surfactant molecule takes part in nanoparticle formation and stabilization [10, 14]. For instance, Sichert et al. demonstrated that the control of surfactant (e.g. *n*-octylamine) amounts during the synthesis process leads to $MAPbBr_3$ with one-, two- or multi- layered nanoplatelets [14]. In contrast, the introduction of surfactants after the formation of $MAPbBr_3$ nanoparticles improves their colloidal stability. Particularly, Kirakosyan et al. [15] and Li et al. [11] showed that the increased surfactant density on nanoparticle surface is characterized by a high photoluminescence quantum yield, and balancing surface passivation and carrier injection via ligand density control increases the external quantum efficiency (EQE) of all-inorganic $CsPbBr_3$ perovskite nanocrystal-based LEDs up to 62.7%. Noteworthy, the surface state has been investigated only when it is partially or completely surfactant covered, while, to best of our knowledge, a bare surface state and the relevant optical properties for $MAPbBr_3$ perovskite nano-sized particles are not fully investigated yet

To date, a limited number of reports on optical properties of $MAPbBr_3$ perovskite nanoparticles with bare surfaces is available since a high surface energy caused the surface activity of nanoparticles leading to their fast deterioration and agglomeration. Bare surface submicron-sized $MAPbBr_3$ particles with a cube shape is reported by Umemoto et al. [16] . The synthesis process is based on the precipitation of precursor solution in a poor solvent, where the poor solvent consist of a mixture of 1,2,4 - trichlorobenzene (TCB) and cyclohexane (CyH) as a non-solvent and good-solvent, respectively. The dissolving ability of the solvent, adjusted by tuning a TCB to CyH ratio, is the key factor to prepare submicron sized cube-shaped perovskite particles with a different size.

In this report, we prepared cub-shaped $MAPbBr_3$ perovskite particles with different edge-size and studied their optical properties depending on particle dimensions. To prepare cube-shaped perovskite particles a surfactant-free precipitation method is applied, where a mixture 1,2,4-trichlorbenzene and cyclohexane is used as poor solvent to precipitate nanocube particles. By adjusting the solvent ratio, we were able to control solvent polarity and perovskite particle size in 100 to 1000 nm range. The PL emission intensity increases along particle size decreases, and the meantime, the excitonic absorption become more distinct. However, non-passivated surface introduces large number of energy trapping sides and significantly effect on photoluminescence quantum yield (PLQY). These findings are of fundamental importance to understand the role of non passivated surface of perovskite crystals on their optical property.

2. Experimental Part

Lead (II) bromide ($PbBr_2$, 99%), *n*-octylamine (≥ 99%), 1,2,4 - trichlorobenzene (99%), and cyclohexane (>99%) were obtained from Aldrich and used without any further purification. Methylamine water solution (CH_3NH_2, 33%), hydrobromic acid (HBr, 48%), toluene (99%), and *N*,*N*-dimethylformamide (99.5%) were received from Daechung Chemicals & Metals. We prepared CH_3NH_3Br separately from commercially available sources such as methylamine water solution and hydrobromic acid. The synthesis reaction was carried out in an ice bath (0°C, 2 h) to effectively remove heat generated by the reaction between amine and acid, thus prevent methylamine evaporation from the reaction vessel. Then the water solvent was evaporated by a rotary evaporator at 40 ~ 45°C. The obtained precipitate was washed with diethyl ether for three times and dried under vacuum (60°C, 6 h) [17].

Submicron sized cube-shaped $CH_3NH_3PbBr_3$ perovskite particles were synthesized by a method reported previously by Umemoto et al. [16] A series of samples were prepared where the solvent environment consists of a mixture of 1,2,4-trichlorbenzene (TCB) and cyclohexane (CyH) with 3:0, 2.5, 0.5, 2:1, 1.5:1.5, 1:2 and 0.5:2.5 ratio, which corresponds to CyH volume contents of 0, 16, 33, 50, 67, and 84%, correspondingly. CyH-x(ratio) notation is introduced for sample nomenclature, where x denotes solvent contents in percent. 60 μL of precursor solution, which consists of 17.3 mg of methylammonium bromide and 56 mg of lead

dibromide dissolved in 5 mL of *N*,*N*-dimethylformamide (DMF), was quickly added into 3 mL of solvent mixture while vigorously stirring. The perovskite nanocubes were formed immediately, which was preliminary identified as colorless solution changed its color to yellow - orange. The solution quickly turned to yellow - orange when only TCB is used, while in the case of high CyH contents, color change occurs relatively slowly. As prepared samples were subjected to spectroscopic examination to obtain optical absorbance and photoluminescence features. UV-vis absorbance spectra (OA) were obtained using Shimadzu UV-2600 spectrophotometer. Photoluminescence (PL) spectra were recorded using Hitachi F-7000 fluorescence spectrometer at room temperature. For the both, absorbance and photoluminescence investigation, we used a quarts cuvette with a 10 mm path length. The samples were diluted twice to avoid high concentration conditioned reabsorption of PL emission. Excitation wavelength of source light (λ_{Exc}) for PLQY measurements was fixed at 365 nm. Photoluminescence quantum yield was measured based on a comparative method by using 9, 10-diphenylanthracene (DPA) as a reference. Photoluminescence decay spectra were obtained using a Fluorolog3 with TCSPC (Horiba Scientific) with a 375 nm laser. To separate the particles for scanning electron microscopy (SEM) and X-ray diffraction examination, the sample were centrifuged at 9000rpm for 15min to collect the particles immediately after synthesis. The supernatant was discard and the precipitate was redispersed in 1 mL of toluene by sonication and drop-casted on Si wafer and glass slide for SEM and XRD, respectively. The phase formation is confirmed by X-ray diffraction method using a Bruker AXS D8 diffractometer with Cu-Kα radiation at λ = 1.54 Å. Hitachi S4800 was used for SEM imaging.

3. Results and Discussion

Figure 1 (a) - (f) shows the SEM images of cube-shaped perovskite particles prepared by tuning the ratio of solvents. In all cases, the particles exhibit a cuboidal shape with well-defined edges and smooth lateral surfaces. Average size of particles increases from 100 nm to 700 nm with increasing CyH content as shown in Figure 1g. Small-sized particles are fairly monodisperse, while big particles are polydisperse where particle size ranged in 300 to

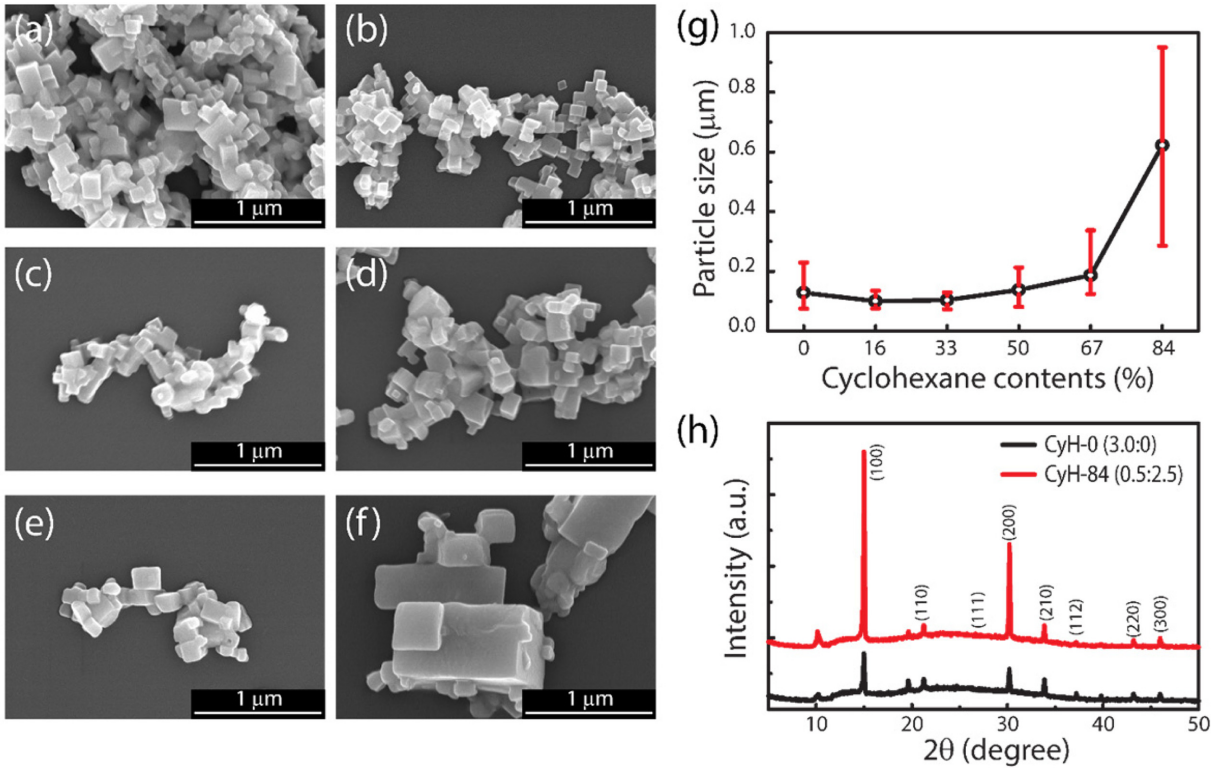

Fig. 1. (a-f) SEM images of cube-shaped perovskite particles prepared by a different ratio of solvents. (g) Particle size as a function of cyclohexane contents. The average size was obtained as an average value of measurement of 25~30 particles. (h) X-ray diffraction pattern for CyH-0 and CyH-84.

1000 nm. X-ray diffraction pattern of CyH-0(3:0) and CyH-84(0.5:2.5) samples (Figure 1h) shows that the synthesized product consists of mainly $MAPbBr_3$, and the crystal structure of $CH_3NH_3PbBr_3$ nanocubes belongs to the space group of *Pm-3m* with a lattice spacing, a = 5.9897 Å regardless of their size. The broadening of the diffraction peaks on the XRD pattern of CyH-0 (3:0) sample corresponds to the size of nanocrystals (80 nm) by the Scherrer formula, which is comparable to that in SEM.

Figure 2 schematically demonstrates the formation mechanism for small and large cube-shape particles for the two distinct cases that pure TCB and 0.5:2.5 ratio of TCB to CyH. In the case of a pure TCB, the solubility of precursor is extremely low since it is a poor solvent. Thus, the supersaturation of precursor reaches quickly and a large number of seeds are created in the solution. The formed seeds grow to small-sized nanocubes (100 ~ 150 nm) because the isotropic growth to all three directions from cubic crystal structure defines the final shape of the particle

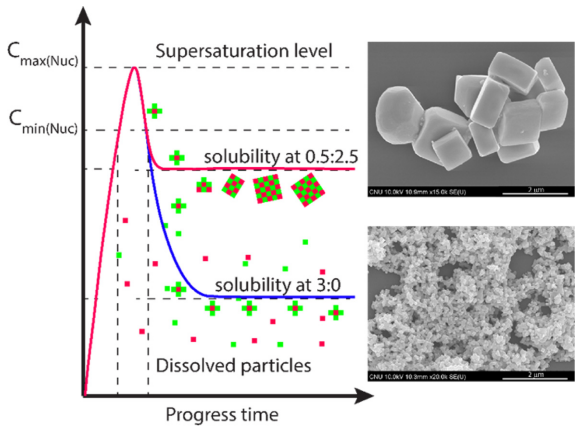

Fig. 2. (a) Scheme of crystal formation and growth for two distinct cases: (b) relatively good solubility and (c) poor solubility with CyH-0 (3:0) and CyH-84 (0.5:2.5) mixing ratio, respectively. Scale bars are 2 μm.

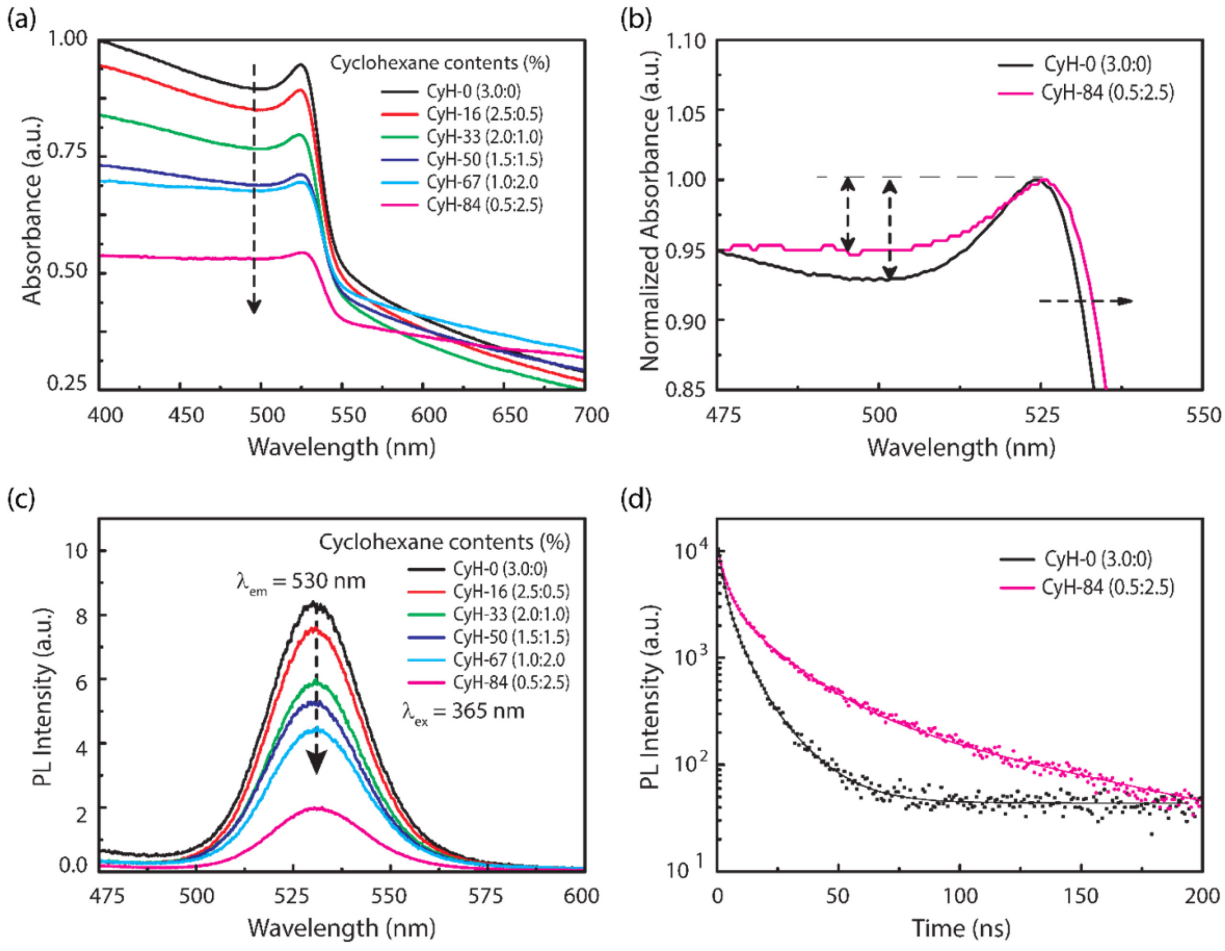

Fig. 3. UV-Vis absorbance shows (a) the absorption features depending on nanocube size and (b) the normalized absorbance for CyH-0 (3:0) and CyH-84 (0.5:2.5) samples corresponding to the smallest and biggest particles. (c) PL emission depending on the cube lateral size at 365 nm excitation. (d) PL decay spectra along with the calculated plot for CyH-0 (3:0) and CyH-84 (0.5:2.5) samples.

to be cuboidal. Increasing the contents of cyclohexane enhances the dissolving ability of solvent mixture, where the supersaturation level is low, and only small number of nuclei are formed. The rest of dissolved precursors in solution provides a necessary building block to the already formed nuclei to grow into much larger-sized crystals reaching up to 1000 nm (Figure 1f). Furthermore, the part of newly formed particles may undergo continuous dissolving process providing an additional source for the bigger particle to grow further (i.e. Ostwald repining process).

Figure 3(a) shows the absorption spectra of $CH_3NH_3PbBr_3$ particles with the different edge size. The UV-vis absorption spectrum of $CH_3NH_3PbBr_3$ nanocrystal has an excitonic band edge at 525 nm (2.36 eV), which is in a good agreement with the literature [1-5]. The normalized absorbance (Figure 3b) shows that their excitonic absorbance is more exhibited for small particles, and decreases as the particle grows. The excitonic absorption is slightly blue-shifted which could be due to the particle growth. Figure 3(c) depicts the photoluminescence emission for the whole series of samples. The PL spectrum peak at 530 nm (2.33 eV) matches to the previously reported data for bulk $CH_3NH_3PbBr_3$ emission wavelength [1-5,12,14]. Stokes shift about ~ 30 meV also indicates that the PL emission originates from excitonic recombination. As the particles size increases, the PL emission intensity gradually (both maximum and integral) decreases. The PLQY determined by the comparative method is in the range of 0.009~0.011%. These bare surface particles exhibit a very low PLQY due to the large number of energy trap sites (i.e. defects) localized on their surface, which is not passivated by any passivating agent such as organic long alkyl chain containing amine, carboxyl, or phosphine type surfactant [15,18]. To understand the effect of energy trapping side we further investigated photoluminescence decay features. Figure 3(d) shows PL decay time for CyH-0 (3:0) and CyH-84 (0.5:2.5) samples. The obtained fluorescent decay curves were well fitted by tri-exponential fitting as follows.

$$I(t) = C + \alpha_1 \exp(-t/\tau_1) + \alpha_2 \exp(-t/\tau_2) + \alpha_3 \exp(-t/\tau_3) \quad (1)$$

$$\tau_{avg} = \frac{\alpha_1 \tau_1^2 + \alpha_2 \tau_2^2 + \alpha_3 \tau_3^2}{\alpha_1 \tau_1 + \alpha_2 \tau_2 + \alpha_3 \tau_3} = f_1 \tau_1 + f_2 \tau_2 + f_3 \tau_3 \quad (2)$$

where $I(t)$ is the intensity, τ is the lifetime, α is the pre-exponential factor, and f is the fractional contribution of each decay component, and C is a constant. The accuracy of the fitting was determined by $\chi^2 = 1 \pm 0.2$ values. The average lifetime (τ_{avg}) values of nanocrystals were derived by eq. 2 [19].

The determined values for decay time and pre-exponential coefficients are in Table 1. Small particles demonstrated fast decay photoluminescence with average lifetime of ($\tau_{avg.}$) 4.6 ns, while larger particles decay slower with longer lifetime of 18.7 ns. Small size particles have a relatively large surface area, and thus higher number of surface defects leads to fast exciton quenching. Lu et al. reported PL decay features for a single crystal of $CH_3NH_3PbBr_3$ where the decay time was increased from 60.1 ns to 345.7 ns after its surface was passivated with $CH_3NH_3PbCl_3$ [20].

4. Conclusions

In conclusion, we have synthesized methylammonium lead tribromide ($CH_3NH_3PbBr_3$) cube-shaped crystals with the edge size ranging from 100 nm to 700 nm by the ligand-free precipitation method, and investigated their optical properties. We have found from the absorption spectra is featured with the excitonic absorption peak, which is well observed for smallest size of particles. In the meantime, the excitonic absorption peak is positioned at the same wavelength for whole range of size and it matches to bulk. Photoluminescence emission is observed at 530 nm for whole range of size of particle. PLQY is 0.009 ~ 0.011%, which is due to energy trapping sites on the surface. Additionally, photoluminescence decay of $CH_3NH_3PbBr_3$ investigation suggest that the fast decay of small size particles compared to big size is due to the large number of surface defects corresponding to energy trapping sites. These findings are of importance for evaluating the surface state on their optical and electronic properties.

Table 1. Parameters used to fit the PL decay curves of the colloidal $CH_3NH_3PbBr_3$ nanoparticles.

	$\tau_{avg.}$	τ_1	α_3	τ_2	α_2	τ_3	α_3	A	χ_2
CyH-0 (3:0)	4.64E-09	5.55E-09	37	1.64E-09	51	1.45E-08	12	4.29E+01	1.0349
CyH-84 (0.5:2.5)	1.22E-08	1.87E-08	32	8.18E-08	5	3.36E-09	63	6.813084	1.2653

Acknowledgements

This study was financially supported by research fund of Chungnam National University.

Competing Financial Interest Statement

The authors declare no competing financial interests.

References

[1] George C. Papavassiliouy, Three- and low-dimensional inorganic semiconductors, Prog. Solid State Chem. 25 (1997) 125-270.

[2] Yupeng Zhang, Jingying Liu, Ziyu Wang, Yunzhou Xue, Qingdong Ou, Lakshminarayana Polavarapu, Jialu Zheng, Xiang Qi, Qiaoliang Bao, Synthesis, properties, and optical applications of low-dimensional perovskites, Chem. Commun. 52 (2016) 13637-13655.

[3] Son-Tung Ha, Rui Su, Jun Xing, Qing Zhang, Qihua Xiong Metal halide perovskite nanomaterials: synthesis and applications, Chem. Sci. 8 (2017) 2522-2536.

[4] He Huang, Lakshminarayana Polavarapu, Jasmina A. Sichert, Andrei S. Susha, Alexander S. Urban, Andrey L. Rogach, Colloidal lead halide perovskite nanocrystals: synthesis, optical properties and applications, NPG Asia Materials 8 (2016) e328.

[5] Mark C. Weidman, Michael Seitz, Samuel D. Stranks, William A. Tisdale, Highly Tunable Colloidal Perovskite Nanoplatelets through Variable Cation, Metal, Halide Composition, ACS Nano 10 (2016) 7830-7839.

[6] Jun Hong Noh, Sang Hyuk Im, Jin Hyuck Heo, Tarak Nathl Mandal, Sang Il Seok, Chemical Management for Colorful, Efficient, and Stable Inorganic-Organic Hybrid Nanostructured Solar Cells, Nano Lett. 13 (2013) 1764-1769.

[7] Ioannis Koutselas, Laurent Ducasse, George C. Papavassiliouy, Electronic properties of three- and low-dimensional semiconducting materials with Pb halide and Sn halide units, J. Phys.: Condens. Matter, 8 (1996) 1217-1227.

[8] Ran Ding, He Liu, Xiaoli Zhang, Juanxiu Xiao, Rahul Kishor, Huaxi Sun, Bowen Zhu, Geng Chen, Fei Gao, Xiaohua Feng, Jingsheng Chen, Xiaodong Chen, Xiaowei Sun, Yuanjin Zheng, Flexible Piezoelectric Nanocomposite Generators Based on Formamidinium Lead Halide Perovskite Nanoparticles, Adv. Funct. Mater. 26 (2016) 7708-7716.

[9] Verena A. Hintermayr, Alexander F. Richter, Florian Ehrat, Markus Döblinger, Willem Vanderlinden, Jasmina A. Sichert, Yu Tong, Lakshminarayana Polavarapu, Jochen Feldmann, Alexander S. Urban, Tuning the Optical Properties of Perovskite Nanoplatelets through Composition and Thickness by Ligand-Assisted Exfoliation, Adv. Mater. 28 (2016) 9478-9485.

[10] Cheng-Hsin Lu, Jiaang Hu, Wan Y. Shih, Wei-Heng Shih, Control of morphology, photoluminescence, and stability of colloidal methylammonium lead bromide nanocrystals by oleylamine capping molecules, J. Colloid Interface Sci 484 (2016) 17–23.

[11] Guangru Li, Florencia Wisnivesky Rocca Rivarola, Nathaniel J. L. K. Davis, Sai Bai, Tom C. Jellicoe, Francisco de la Peña, Shaocong Hou, Caterina Ducati, Feng Gao, Richard H. Friend, Neil C. Greenham, Zhi-Kuang Tan, Highly Efficient Perovskite Nanocrystal Light-Emitting Diodes Enabled by a Universal Crosslinking Method, Adv Mater 29 (2017) 1603885.

[12] Sung-Hoon Kim, Artavazd Kirakosyan, Jihoon Choi, Jong H. Kim, Detection of volatile organic compounds (VOCs), aliphatic amines, using highly fluorescent organic-inorganic hybrid perovskite nanoparticles, Dyes Pigm 147 (2017) 1-5.

[13] Chinnadurai Muthu, Sunena R. Nagamma, Vijayakumar C. Nair, Luminescent hybrid perovskite nanoparticles as a new platform for selective detection of 2,4,6-trinitrophenol, RSC Adv. 4 (2014) 55908-55911.

[14] Jasmina A. Sichert, Yu Tong, Niklas Mutz, Mathias Vollmer, Stefan Fischer, Karolina Z. Milowska, Ramon García Cortadella, Bert Nickel, Carlos Cardenas-Daw, Jacek K. Stolarczyk, Alexander S. Urban, Jochen Feldmann, Quantum Size Effect in Organometal Halide Perovskite Nanoplatelets. Nano Lett. 15 (2015) 6521-6527.

[15] Artavazd Kirakosyan, Seokjin Yun, Soon-Gil Yoon, Jihoon Choi, Surface Engineering for Improved Stability of $CH_3NH_3PbBr_3$ Perovskite Nanocrystals, Nanoscale, (2017) DOI: 10.1039/C7NR06547G.

[16] Kazuki Umemoto, Yong-Jin Pu, Cigdem Yumusak, Markus Clark Scharber, Matthew Schuette White, Niyazi Serdar Sariciftci, Tsukasa Yoshida, Jun Matsui, Hiroshi Uji-I, Akito Masuhara, Size control of $CH_3NH_3PbBr_3$ perovskite cuboid fine crystals synthesized by ligand-free reprecipitation method, Microsyst. Technol. 6 (2017) 1-5.

[17] Artavazd Kirakosyan, Jiye Kim, Sung Woo Lee, Ippili Swathi, Soon-Gil Yoon, Jihoon Choi, Optical Properties of Colloidal $CH_3NH_3PbBr_3$ Nanocrystals

by Controlled Growth of Lateral Dimension, Cryst. Growth Des, 17 (2017) 794-799.

[18] B. O. Dabbousi, J. Rodriguez-Viejo, F. V. Mikulec, J. R. Heine, H. Mattoussi, R. Ober, K. F. Jensen, M. G. Bawendi, (CdSe)ZnS Core−Shell Quantum Dots: Synthesis and Characterization of a Size Series of Highly Luminescent Nanocrystallites, J. Phys. Chem. B 101 (1997) 9463-9475.

[19] J.R. Lakowicz, Principles of Fluorescence Spectroscopy, Third Edition, Baltimore, Maryland, USA, (2006).

[20] Haizhou Lu, Huotian Zhang, Sijian Yuan, Jiao Wang, Yiqiang Zhan, Lirong Zheng, An optical dynamic study of $MAPbBr_3$ single crystals passivated with $MAPbCl_3/I_3$-$MAPbBr_3$ heterojunctions, Phys. Chem. Chem. Phys 19 (2017) 4516-4521.